Arab J. Nucl. Sci. Appl., Vol. 56, 1, 1-8 (2023)

ISSN 1110-0451

Arab Journal of Nuclear Sciences and Applications

Web site: ajnsa.journals.ekb.eg

(E S N S A)

Radon Measurement and Radiological Dose Assessment from Terrestrial Rocks Using Solid-State Nuclear Track Detectors

M. Mitwalli [1,2*], W. Badawy [3,4], H. Yousef [5], S. Salama[3], G. Saleh[6], A. H. El-Farrash[1]

[(1)] *Physics Department, Faculty of Science, Mansoura University, 35516 Mansoura, Egypt*
[(2)] *National Network for Nuclear Sciences, Academy of Scientific Research and Technology (NNS-ASRT), 11334 Cairo, Egypt*
[(3)] *Egyptian Atomic Energy Authority, Nuclear Research Center, Radiation Protection and Civil Defense Department, 13759, Cairo, Egypt*
[(4)] *Joint Institute for Nuclear Research (FNPL-JINR), 141980, Dubna, Russian Federation*
[(5)] *Physics Department, Faculty of Science, Suez University, Suez, Egypt*
[(6)] *Nuclear Materials Authority (NMA), El-Maadi, P.O. Box 530, Cairo, Egypt*

HIGHLIGHTS

1. Radiometric and radiological studies of the Sukari granitoid pluton with SSNTDs were performed.
2. Significant levels of radioactivity were detected in the studied areas.
3. The results of radon radioactivity were mapped and the areas with peak values were identified.
4. The noticeable levels of radioactivity pose a significant risk to humans and the environment.

GRAPHICAL ABSTRACT

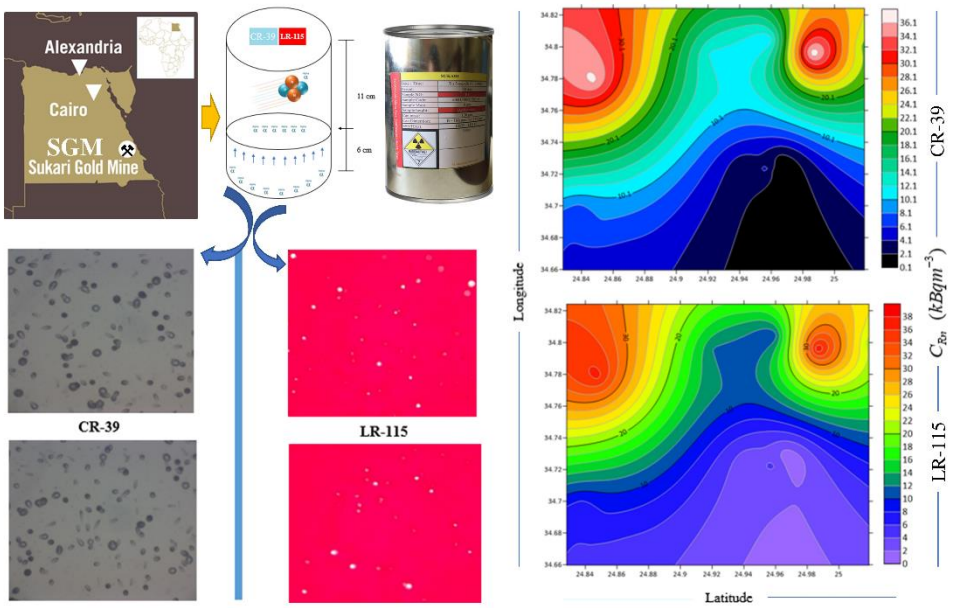

ARTICLE INFO

Article history:

Received: 12th May 2022
Accepted: 25th Aug. 2022

Keywords:

Sukari Gold Mine;
Radon;
SSNTDs;
Radiological Hazards;
Annual Dose,
Radioactivity.

ABSTRACT

The Sukari granitoid pluton, namely the Sukari gold mine (SGM), located in Egypt's southeastern desert, is outstanding gold-bearing granite in the Arabian Nubian Shield. CR-39 and LR-115 Nuclear Track Detectors (NTD) were used in the present study to determine radon concentration, after which the exhalation rate, annual effective dose, and work level were calculated. The overall average radon values from the CR-39 and LR-115 NTD are 11.27 and 11.29 kBqm^{-3}, respectively, indicating a consensual correlation that depends on the charged particles, particularly accumulation radon gas emissions from investigated samples measured by Nuclear Track Detectors. The findings revealed a significant quantity of NORM in the SGM due to the radon concentration which is greater than the IAEA, ICRP, and UNSCEAR recommended limit of 1000 Bqm^{-3}. The present study aims to evaluate and predict the radioactive changes in the investigation area, assess dangerous radiation, and implement radiation safety standards for the workers in the SGM. The current research may also be useful in the future investigation and mining of nuclear materials for optimization business in the SGM and its surrounding area.

Corresponding author: meto_mms@yahoo.com
DOI: 10.21608/ajnsa.2022.138031.1581

INTRODUCTION

Internal radiation doses in the human body are derived from inhalation of radioactive gases, particularly radon and thoron gases, and incorporation of multi-radionuclides which are the primary routes by which radioactive isotopes enter the human body [1,2]. Because an alpha decay chain of ^{226}Ra produces ^{222}Rn in sediment, soil, and rocks, it is gaseous decay in this series as a noble gas, accounting for a portion of the ^{222}Rn discharged into the atmosphere. The human population has a detrimental effect due to radon radiation, which poses a possible threat [3]. Solid-State Nuclear Track Detectors (SSNTDs) emulsion sheet is utilized significantly in the different environmental monitoring investigations and assessment of charged particles. Radionuclides always exist on Earth's surface and are affected by the natural geological structure. The distribution of radioactive nuclides is associated with geochemical and geographical aspects of location, with varying magnitudes of the environmental process concerning strike-slip sheared zones, thrusts, folds, attitude/plunge of alienation, major fractures, and orogenic strike-slip faults that occur sequentially as shown in the geological map of Figure (1), as well as ongoing drilling and exploration work at the Sukari gold mine. All of the aforementioned make a noticeable change in the background, which prompted the study to monitor the radioactivity and assess the radiological impact [2, 4]. Among the natural radionuclides and different isotopes of radon, the present study is interested in ^{222}Rn, which decays with a half-life of 3.82 days into many short-lived but highly alpha emitter daughter progenies including ^{218}Po and ^{214}Po.

The determination of radon concentrations is very important due to the health risk and design of the control strategies and the hazard for occupational radiation exposure in the Sukari Gold Mine Area (SGMA), Southeastern Desert, Egypt. Mining and prospecting for gold in SGMA requires deep digging operations and whose originators produce huge amounts of rocks after separating gold ore from rocks which are stored without use. Thus, the study is directed to benefit from these large and unused quantities of rocks. The SGMA is situated about 30 km Southwest-Marsa Alam within the Precambrian rocks of the Southeastern Desert of Egypt. SGMA is characterized by an arc structure with Northwest –Southeast trend in the south and Northeast–Southwest direction in the north [5].

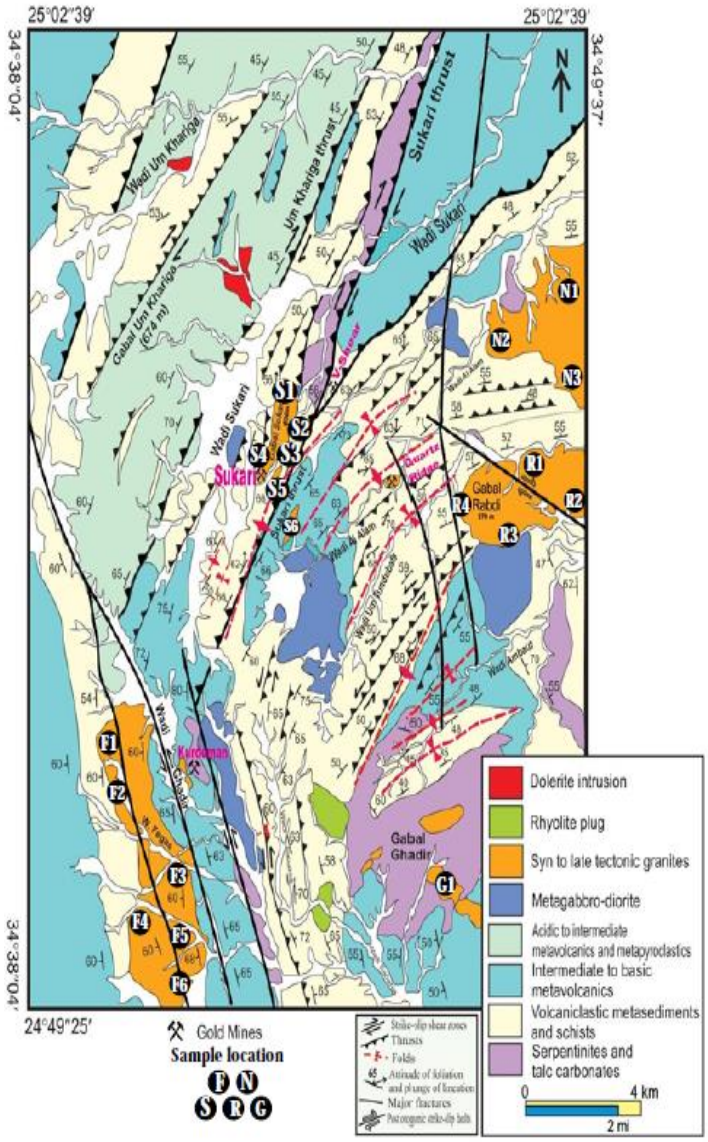

Fig. (1): The geological map of the collected samples of SGMA, Egypt [5, 6]

In terms of the geological background of the SGMA, the samples obtained comprised Mafic-ultramafic Ophiolitic Rocks, Island Arc-related, Volcaniclastic, Metasediments-plutonic, Assemblages, and Syn-Orogenic Intrusions. They are made up of medium to Coarse-grained Alkali-feldspar Granite, Younger Granite, and Monzogranite that have intruded the Volcano-sedimentary, sequences Metagabbro-diorite complex. Dolerite, Diorite, and Felsic Dikes subsequently cut all of these rocks. The Sukari area's Ophiolitic suite is fragmented and consists of Serpentinite-talc-carbonate and Metagabbro-diorite complexes. During an Island Arc stage, this Ophiolitic suite was overlain by Volcaniclastic Metasediments and subsequently intruded by Sukari Granites. Contacts

between Serpentinite-talc-carbonate rocks and surrounding country rocks are Tectonic, while connections between Serpentinite-talc-carbonate rocks and Metagabbro-diorite are gradational. The Volcaniclastic Metasediments are the most common rock units in the current region. This unit comprises mature Island Arc Assemblages of Meta-volcanic, Meta-pyroclastic, and very thick and widespread schists. The geological map of SGMA and the distribution pattern of examined materials are shown in Figure (1).

The current work is interested in assessing radon concentration and its radiological impact to detect background radioactivity levels that can help protect workers from hazards and monitor the change parallel to the geological process in the area dependent on mining operations in the SGMA.

Sampling and experimental methods

A research project to monitor environmental radiation is concerned with conducting a radiological survey of important areas such as mines and quarries to produce ores and minerals. It is worth noting that the project began its activities in 2020 to the present time. The study was concerned with gold mines, and twenty samples were collected from various places inside and around the SGMA.

According to the drilling work and mining process, the investigated samples have been taken within the mine from a certain depth ranging from surface to 5 meters. In addition, some samples have been collected from the residual material stored after gold extraction, taking the geological features into chronology as shown in Figure (1) which illustrates the distribution pattern of the collected samples. The sampling strategy followed the Egyptian Geological Survey and Mining Authority standards and IAEA guidelines for the environmental pollutants. The weight of the samples was restricted to about 400 gm, which is a closely monitored effective volume and geometric closed-can technique, and Figure (2) shows an example for the collected samples. The samples were collected using the closed-can method to quantify radon concentrations and exhalation rates using SSNTDs.

All investigated samples were dried in an oven at 110°C for 3 hours, sieved through one mesh, and weighed before being sealed for 50 days in a closed cylindrical stainless-steel container. The specified can have a geometric size of 10.6 cm in diameter, 17 cm in height, and a density of 7620 kgm^{-3}. The containers were firmly sealed with an inverted cylindrical metal cover. The free space between the surface of the sample and the installed polymer detectors was 11 cm to standardize the height of the stored samples within the sealed can as shown in Figure (3) which presents a diagram of the irradiation process of the SSNTDs with alpha particles emitted from the investigated samples. The CR-39 and LR-115 detectors, each having an area of 1.5 cm, were mounted at the bottom center of each inverted metal cover.

Fig. (2): Actual collected sample of Sukari gold Mine, Egypt

The CR-39 and LR-115 NTD were carefully removed from the can after 27 days of irradiation duration, indicating that the degradation of ^{226}Ra secular equilibrium had occurred. when long radioactive half-lives, ^{238}U and ^{234}U isotopes are in secular equilibrium in all minerals and rocks greater than one million years old in a closed system or undisturbed minerals since ^{234}U is a daughter product of ^{238}U and the activity ratio (AR) of ^{234}U to ^{238}U is unity in the bulk of such materials. However, when such rocks, sediments and minerals have interacted with hydrothermal and geochemical activity in addition to ongoing drilling and exploration work. the ratio may deviate from unity on either side; disequilibrium is the result depending on the geochemical conditions therefore the atypical deformation rebalanced [7-11]. For 8 hours, the CR-39 NTD was etched in a 6.25N NaOH solution at 70±1°C. The CR-39 NTD were rinsed in distilled water after etching and then submerged for several minutes in a 3 percent acetic acid solution; thenthey have been cleaned again in distilled water and dried [10, 12-14].

The LR-115 detectors were etched in NaOH 2.5N for 2 hours in a water bath at 60±1°C. Following chemical etching, the LR-115 NTD were washed with distilled water and placed in 50 mL of ethyl alcohol, followed by 50 mL of distilled water. They were then washed with distilled water again and dried in air.

The CR-39 and LR-115 detectors' Alpha tracks were counted using a 640^{x} optical microscope after they were etched. For the actual summation of alpha tracks, both SSNTDs' backgrounds were counted and subtracted from the overall count [12, 14, 15].

The following equation gives the radon concentration C_{Rn} in Bqm^{-3} at secular equilibrium [7-11]:

$$C_{Rn} = \frac{\rho}{\eta T} \pm \frac{\sqrt{\frac{\alpha}{f \pi r^2}}}{\eta T} \quad \textbf{(1)}$$

Where ρ is the track density (tracks/cm^2) and it is calculated by the following relation [14]:

$$\rho = \frac{\alpha}{f \pi r^2} \pm \sqrt{\frac{\alpha}{f \pi r^2}} \quad \textbf{(2)}$$

Where α is the actual summation of Alpha tracks, f is the number of the investigated fields, πr^2 is the calibrated area of the studied fields, T is the initializing irradiation period (27 days), and η is the calibration coefficient of CR-39 and LR-115 detectors [10, 14].

The radon surface exhalation rate E_A is given by the relation:

$$E_A = \frac{C_{Rn}\, V \lambda}{A[T + \frac{1}{\lambda}(e^{-\lambda T} - 1)]} \pm \frac{\sqrt{\frac{\alpha}{f \pi r^2}}\, V \lambda}{\eta T A[T + \frac{1}{\lambda}(e^{-\lambda T} - 1)]} \quad \textbf{(3)}$$

Where E_A is exhalation rate (Bqm^{-2}h^{-1}), λ is the radon decay constant (0.00756 h^{-1}), C_{Rn} is the radon concentration (Bqm^{-3}), V is the effective volume of Can (m^3), A is the cross-sectional area (m^2), and T is the initializing irradiation period (27 days) [16-18].

The following equation was used to compute the annual effective dose D_E:

$$D_E = AHFTC_{Rn} \pm \frac{AHFT\sqrt{\frac{\alpha}{f \pi r^2}}}{\eta T} \quad \textbf{(4)}$$

Where A is the conversion factor of the annual effective dose (9×10^{-6} mSvh^{-1} / Bqm^{-3}), H is the indoor occupancy factor (0.8), F=0.4 is the indoor equilibrium factor between radon and its progeny [4, 11, 19-21], and T is the indoor exposure time in hours per year which equals 2000 hy^{-1} [4, 18].

The working levels are calculated using the following equation [22]:

$$WL = \frac{C_{Rn}\, x\, f}{3700} \pm \frac{\sqrt{\frac{\alpha}{f \pi r^2}}\, x\, f}{\eta T\, x\, 3700} \quad \textbf{(5)}$$

Where C_{Rn} is radon concentration in Bqm^{-3}, f is the equilibrium factor for radon that has been taken as 0.4 by ICRP [4, 11, 19-21], and 3700 is the conversion factor to working levels [4, 11, 23].

Fig. (3): Set-up system used to determine radon concentrations

RESULTS AND DISCUSSION

The present investigation reveals that the radon concentration values obtained from the CR-39 and LR-115 detectors are comparable, owing to the energy window of each NTD, as shown in Figure (2). The NTD radon concentration values for CR-39 and LR-115 varied from 0.68±0.02 to 37.75±0.17 kBqm^{-3}, with an average value of 11.30±0.08 kBqm^{-3}. The radon concentration fluctuates from sample to sample according to the geological processes such as strike-slip sheared zones, thrusts, folds, alienation attitude/plunge, significant fractures, and orogenic strike-slip faults that occur consecutively, as well as continuing drilling and exploratory operations. This is in addition to the geochemical structure of the collected samples (intermediate to basic Metavolcanics, Volcaniclastic Metasediments, Schists, Serpentinites, and Talc Carbonates).

Table (1) shows the radon concentrations and exhalation rate of the investigated samples by CR-39 and LR-115 detectors. It is noted that radon activity concentrations are greater than 1000 Bqm^{-3}, which is higher than the permissible range and world limit recommended by ICRP, IAEA [15, 24, 25].

Table (1): Radon concentration and exhalation rate values for *SGMA*.

Sample	C_{Rn} (kBqm^{-3})		E_A (Bqm^{-2}h^{-1})	
	CR-39	LR-115	CR-39	LR-115
S.1	0.68 ± 0.02	0.68 ± 0.05	0.08 ± 0.02	0.08 ± 0.04
S.2	1.18 ± 0.03	1.12 ± 0.07	0.14 ± 0.01	0.13 ± 0.01
S.3	1.93 ± 0.04	3.85 ± 0.12	0.23 ± 0.01	0.46 ± 0.02
S.4	4.43 ± 0.06	4.24 ± 0.13	0.53 ± 0.01	0.51 ± 0.02
S.5	4.13 ± 0.06	4.07 ± 0.13	0.5 ± 0.03	0.49 ± 0.07
S.6	2.50 ± 0.04	2.44 ± 0.10	0.3 ± 0.02	0.29 ± 0.06
F.1	4.67 ± 0.06	4.42 ± 0.13	0.56 ± 0.01	0.53 ± 0.02
F.2	4.65 ± 0.06	4.69 ± 0.14	0.56 ± 0.01	0.56 ± 0.03
F.3	6.01 ± 0.07	6.04 ± 0.16	0.72 ± 0.03	0.73 ± 0.07
F.4	7.88 ± 0.08	7.62 ± 0.18	0.95 ± 0.01	0.92 ± 0.02
F.5	7.07 ± 0.08	7.14 ± 0.17	0.85 ± 0.02	0.86 ± 0.05
F.6	6.56 ± 0.07	6.56 ± 0.16	0.79 ± 0.01	0.79 ± 0.03
R.1	10.57 ± 0.09	10.37 ± 0.20	1.27 ± 0.02	1.25 ± 0.04
R.2	17.9 ± 0.12	17.81 ± 0.27	2.15 ± 0.01	2.14 ± 0.03
R.3	11.88 ± 0.10	11.77 ± 0.22	1.43 ± 0.01	1.42 ± 0.02
R.4	11.85 ± 0.10	11.71 ± 0.22	1.43 ± 0.01	1.41 ± 0.02
N.1	21.27 ± 0.13	21.29 ± 0.29	2.56 ± 0.00	2.56 ± 0.01
N.2	25.84 ± 0.14	25.71 ± 0.32	3.11 ± 0.01	3.09 ± 0.03
N.3	37.75 ± 0.17	37.63 ± 0.39	4.54 ± 0.02	4.53 ± 0.05
G.1	36.68 ± 0.17	36.68 ± 0.38	4.41 ± 0.02	4.41 ± 0.04
Ava.	**11.27**	**11.29**	**1.36**	**1.36**
Max.	**37.75**	**37.63**	**4.54**	**4.53**
Min.	**0.68**	**0.68**	**0.08**	**0.08**
S. D.	**11.11**	**11.03**	**1.34**	**1.33**

As for the surface exhalation rate, the result values ranged from 0.30 to 4.54 Bqm^{-2}h^{-1} with an average value of 1.36±0.01 Bqm^{-2}h^{-1}. The annual effective dose varied from 3.9 to 217.47 mSvy^{-1} with an average value of 64.92±0.70 mSvy^{-1}, as shown in Table (2), which is higher than the permitted dose of 20 mSvy^{-1} recommended by the ICRP and UNSCEAR [21, 24]. The work level values ranged from 0.07 to 4.07 with an average value of 1.22±0.03 kBqm^{-3}. Table (3) shows the permissible dose limit corresponding to radon gas exposure and its product druthers.

Table (2): Annual effective dose and work level values for *SGMA*

Sample	D_E (mSvy^{-1})		W_L (kBqm^{-3})	
	CR-39	LR-115	CR-39	LR-115
S.1	3.90 ± 0.81	3.93 ± 1.84	0.07 ± 0.02	0.07 ± 0.03
S.2	6.78 ± 0.31	6.42 ± 0.72	0.13 ± 0.01	0.12 ± 0.01
S.3	11.13 ± 0.50	22.15 ± 1.06	0.21 ± 0.01	0.42 ± 0.02
S.4	25.50 ± 0.27	24.44 ± 0.74	0.48 ± 0.01	0.46 ± 0.01
S.5	23.76 ± 1.42	23.42 ± 3.13	0.45 ± 0.03	0.44 ± 0.06
S.6	14.40 ± 1.18	14.07 ± 2.64	0.27 ± 0.02	0.26 ± 0.05
F.1	26.89 ± 0.39	25.45 ± 0.90	0.5 ± 0.01	0.48 ± 0.02
F.2	26.76 ± 0.67	27.02 ± 1.44	0.5 ± 0.01	0.51 ± 0.03
F.3	34.60 ± 1.41	34.78 ± 3.16	0.65 ± 0.03	0.65 ± 0.06
F.4	45.41 ± 0.49	43.91 ± 1.14	0.85 ± 0.01	0.82 ± 0.02
F.5	40.72 ± 1.09	41.14 ± 2.46	0.76 ± 0.02	0.77 ± 0.05
F.6	37.77 ± 0.61	37.76 ± 1.37	0.71 ± 0.01	0.71 ± 0.03
R.1	60.88 ± 0.76	59.73 ± 1.72	1.14 ± 0.01	1.12 ± 0.03
R.2	103.12 ± 0.56	102.60 ± 1.27	1.94 ± 0.01	1.93 ± 0.02
R.3	68.45 ± 0.52	67.81 ± 1.17	1.28 ± 0.01	1.27 ± 0.02
R.4	68.28 ± 0.34	67.47 ± 0.82	1.28 ± 0.01	1.27 ± 0.02
N.1	122.54 ± 0.23	122.60 ± 0.72	2.3 ± 0.00	2.3 ± 0.01
N.2	148.81 ± 0.62	148.08 ± 1.30	2.79 ± 0.01	2.78 ± 0.02
N.3	217.47 ± 0.98	216.72 ± 2.22	4.08 ± 0.02	4.07 ± 0.04
G.1	211.27 ± 0.78	211.25 ± 1.74	3.97 ± 0.01	3.96 ± 0.03
Ava.	**64.92**	**65.04**	**1.22**	**1.22**
Max.	**217.47**	**216.72**	**4.08**	**4.07**
Min.	**3.90**	**3.93**	**0.07**	**0.07**
S. D.	**64.02**	**63.55**	**1.2**	**1.19**

In all European nations, the allowable effective dosage from occupational radiation dose is 20 mSvy^{-1}, whereas, in the United States, it is 50 mSvy^{-1}. In this regard, the obtained results are in agreement with the literature published data for the similar environment of different countries [3, 13, 26-36]. Figure (4) shows a comparison between radon concentration results for NTD, sample (N3) that has a high value of radon concentration due to increasing content of ^{238}U and ^{226}Ra activity concentration; on the other hand, sample coded (S1) has a low value of radon concentration due to low level of ^{238}U.

Table (3): Radon gas concentration for different countries and organizations

Limitation							
R*	(Bqm^{-3})	R*	(Bqm^{-3})	R*	(Bqm^{-3})	R*	(Bqm^{-3})
WHO	100	Russia	200	Germany	250	ICRP	400
USA	150	Australia	200	Luxemburg	250	France	400
India	150	Ireland	200	Turkey	400	Canada	800
Norway	200	China	200	EU	400	UNSCEAR	800
UK	200	Sweden	200	Denmark	400	IAEA	1000
R* = Reference of permissible limit dose							

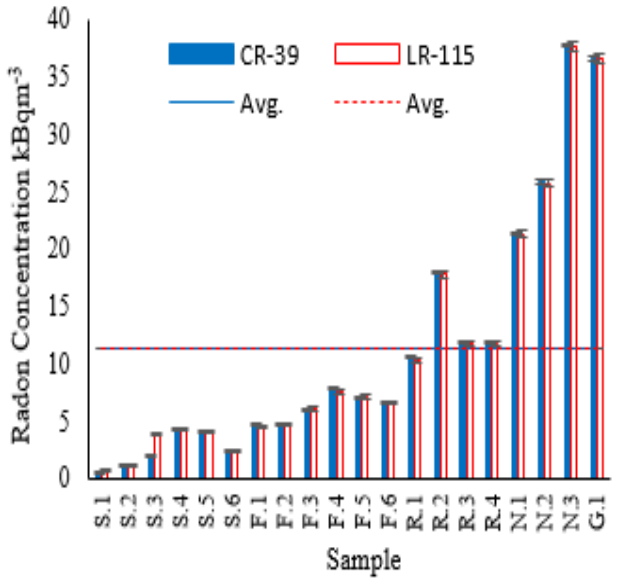

Fig. (4): Comparison between radon concentration results of both CR-39 and LR-115 NTD

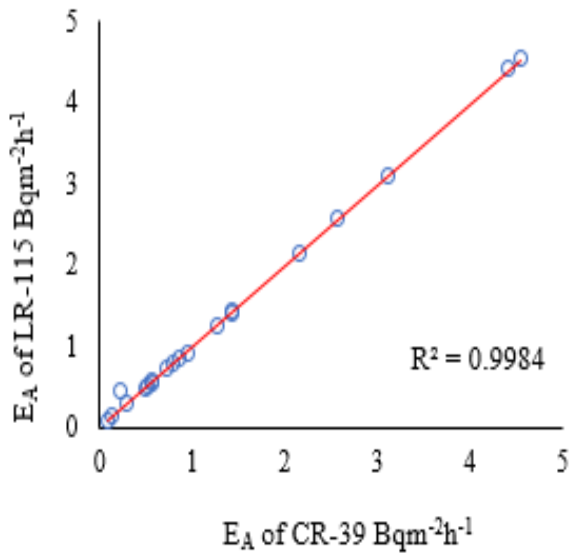

Fig. (5): Correlation relation between average radon concentration values and surface exhalation of *NTD*

Figure (5) shows the correlation between radon concentration and the surface exhalation rate, which indicates a significant agreement between C_{Rn} measurement and E_A related to the typical effective volume of the container, the surface area of the sample, and the radon decay constant. These affect the exhalation rate have given. Radon exhalation is significant for determining the relative contribution of the material to the overall radon concentration observed and for related health risks associated with radon. The measurement results have been fed to the Surfer® software, and contour maps of Figures (6) which have been drawn to track radon concentration on the function of the coordinates for the collected samples from SGMA.

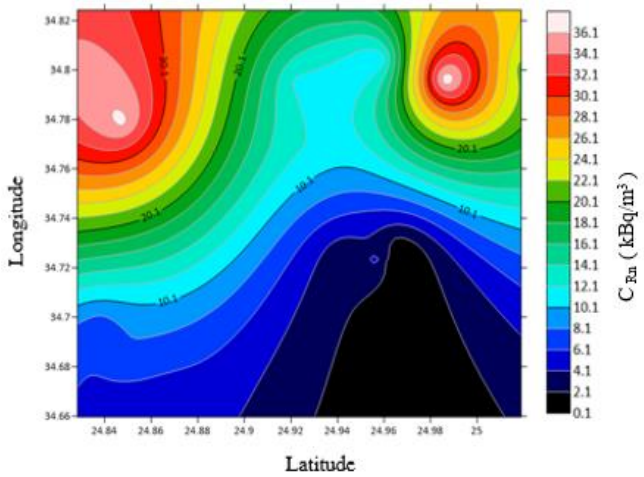

Fig. 6 (A): Contour map of radon concentration using CR-39 NTD as the geographical coordinates of the collected samples

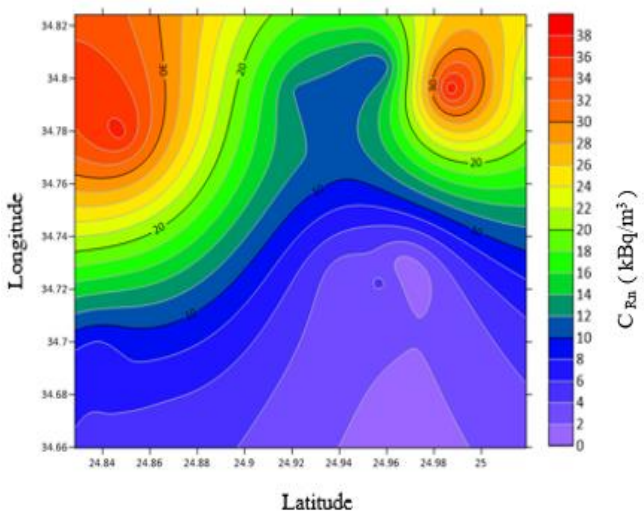

Fig. 6 (B): Contour map of radon concentration using LR-115 NTD as the geographical coordinates of the collected samples

CONCLUSIONS

The present study of the Sukari gold mines region determined that it is significantly polluted with radon concentrations due to the geological makeup of numerous rocks and geochemical processes which occur consecutively in the Sukari gold mine and the nearby places. The result of this study will help determine the locations with the highest and lowest levels of radon concentration in the SGMA, as well as identified fluctuations in the concentration of radioactive radionuclides that affect the environment of SGMA. Radon concentrations are often higher than the recommended threshold by ICRP and UNSCEAR (1000 Bqm^{-3}) as it is frequently greater than the ICRP's occupational reference level (1500 Bqm^{-3}). The data produced records the radioactivity background levels in rock samples and may be used as reference information in the SGMA to detect any radioactive background level changes caused by geological activity in the area. Contour maps may be used to track changes in environmental radioactivity by monitoring the distribution of radon concentrations. The SGMA investigated samples and stations analyzed to serve as the basis for future elemental composition studies using neutron activation analysis to explore heavy and rare elements. Furthermore, the study estimate the equivalent content of uranium and thorium as a source of radon isotopes, moreover will be very valuable if the research is related to nuclear material exploration.

REFERENCES

[1] Misdaq, M.A. and A. Mortassim, *222RN and 220RN concentrations measured in various natural honey samples by using nuclear track detectors and resulting radiation doses to the members of the rural populations in Morocco.* Radiat Prot Dosimetry, 2008. **130**(1): p. 115-8.

[2] Kumar, G., et al., *Radioactivity monitoring in the vicinity of Jawalamukhi thrust NW Himalaya, India for tectonic study*. Natural Hazards, 2022: p. 1-22.

[3] Przylibski, T.A., *Radon and its daughter products behaviour in the air of an underground tourist route in the former arsenic and gold mine in Złoty Stok (Sudety Mountains, SW Poland).* J Environ Radioact, 2001. **57**(2): p. 87-103.

[4] UNSCEAR, *Sources and Effects of Ionizing Radiation*, ed. R.t.t.G. Assembly. Vol. 1. 2000, New York: United Nations Scientific Committee on the Effects of Atomic Radiation.

[5] Abd El-Wahed, M.A., H. Harraz, and M.H. El-Behairy, *Transpressional imbricate thrust zones controlling gold mineralization in the Central Eastern Desert of Egypt.* Ore Geology Reviews, 2016. **78**: p. 424-446.

[6] Abd El-Wahed, M.A., *Oppositely dipping thrusts and transpressional imbricate zone in the Central Eastern Desert of Egypt.* Journal of African Earth Sciences, 2014. **100**: p. 42-59.

[7] Tripathi, R.M., et al., *Study of uranium isotopic composition in groundwater and deviation from secular equilibrium condition.* Journal of Radioanalytical and Nuclear Chemistry, 2013. **295**(2): p. 1195-1200.

[8] Todd, D.K. and L.W. Mays, *Groundwater hydrology*. 2004: John Wiley & Sons.

[9] Ivanovich, M., *Uranium series disequilibrium: applications to environmental problems*. 1982: Clarendon Press.

[10] Abbas, Y.M., et al., *Measurement of 226Ra concentration and radon exhalation rate in rock samples from Al-Qusair area using CR-39.* Journal of Radiation Research and Applied Sciences, 2020. **13**(1): p. 102-110.

[11] IAEA, *Analytical Methodology for the Determination of Radium Isotopes in Environmental Samples*. 2011, Vienna: International Atomic Energy Agency.

[12] Yousef, H.A., et al., *Radon exhalation rate for phosphate rocks samples using alpha track detectors.* Journal of Radiation Research and Applied Sciences, 2016. **9**(1): p. 41-46.

[13] Saleh, G.M., et al., *Environmental Radioactivity of Radon and its Hazards in Hamash Gold Mine, Egypt.* Arab Journal of Nuclear Sciences and Applications, 2019. **52**(4): p. 190-196.

[14] Saleh, G.M., et al., *Environmental Radioactivity of Radon and its Hazards in Hamash Gold Mine, Egypt.* Arab Journal of Nuclear Sciences and Applications, 2019. **52**(4): p. 190-196.

[15] Singh, S. and S. Prasher, *The etching and structural studies of gamma irradiated induced effects in CR-39 plastic track recorder*. Nuclear Instruments and Methods in Physics Research Section B: Beam Interactions with Materials and Atoms, 2004. **222**(3): p. 518-524.

[16] Shafi ur, R., et al., *Determination of 238U contents in ore samples using CR-39-based radon dosimeter—disequilibrium case.* Radiation Measurements, 2006. **41**(4): p. 471-476.

[17] Barooah, D. and P.P. Gogoi, *Study of radium content, radon exhalation rates and radiation doses in solid samples in coal-mining areas of Assam and Nagaland using LR-115 (II) nuclear track detectors*. 2019, India: Vishal Publishing Company.

[18] El-Farrash, A.H., H.A. Yousef, and A.F. Hafez, *Activity concentrations of 238U and 232Th in some soil and fertilizer samples using passive and active techniques.* Radiation Measurements, 2012. **47**(8): p. 644-648.

[19] UNSCEAR, *Report of the United Nations Scientific Committee on the Effects of Atomic Radiation* UNSCEAR, 2011. **58**: p. 12.

[20] ICRP, *Protection Against Radon-222 at Home and at Work*. 1993, ICRP. p. . Ann. ICRP 23 (2).

[21] ICRP, *Human Respiratory Tract Model for Radiological Protection*, I.P. 66, Editor. 1994, ICRP.

[22] Abu-Jarad, F.A., *Application of nuclear track detectors for radon related measurements.* International Journal of Radiation Applications and Instrumentation. Part D. Nuclear Tracks and Radiation Measurements, 1988. **15**(1-4): p. 525-534.

[23] IAEA, *National and Regional Surveys of Radon Concentration in Dwellings*. 2014, Vienna: International Atomic Energy Agency.

[24] ICRP, *Recommendations of the International Commission on Radiological Protection*, I. Publication, Editor. 1991, ICRP.

[25] IAEA, *Radiation Protection against Radon in Workplaces other than Mines*. 2004, Vienna: INTERNATIONAL ATOMIC ENERGY AGENCY.

[26] Ielsch, G., et al., *study of a predictive methodology for quantification and mapping of the radon-222 exhalation rate.* Journal of Environmental Radioactivity, 2002. **63**(1): p. 15-33.

[27] Speelman, W.J., et al. *Radon generation and transport in and around a gold mine tailings dam in South Africa*. in *Second European IRPA congress on radiation protection - Radiation protection: from knowledge to action*. 2006. France.

[28] Somlai, J., et al., *Radon concentration in houses over a closed Hungarian uranium mine.* Science of The Total Environment, 2006. **367**(2): p. 653-665.

[29] Szegvary, T., M.C. Leuenberger, and F. Conen, *Predicting terrestrial ²²²Rn flux using gamma dose rate as a proxy.* Atmos. Chem. Phys., 2007. **7**(11): p. 2789-2795.

[30] Mahur, A.K., et al., *Measurement of natural radioactivity and radon exhalation rate from rock samples of Jaduguda uranium mines and its radiological implications.* Nuclear Instruments and Methods in Physics Research Section B: Beam Interactions with Materials and Atoms, 2008. **266**(8): p. 1591-1597.

[31] Zhuo, W., et al., *Estimating the amount and distribution of radon flux density from the soil surface in China.* J Environ Radioact, 2008. **99**(7): p. 1143-8.

[32] Hirao, S., H. Yamazawa, and J. Moriizumi, *Inverse modeling of Asian 222Rn flux using surface air 222Rn concentration.* Journal of Environmental Radioactivity, 2010. **101**(11): p. 974-984.

[33] Rana, B.K., et al., *Assessment of radon concentration and external gamma radiation level in the environs of Narwapahar uranium mine, India and its radiological significance.* Journal of Radioanalytical and Nuclear Chemistry, 2011. **290**(2): p. 347-352.

[34] Grossi, C., et al., *Inter-comparison of different direct and indirect methods to determine radon flux from soil.* Radiation Measurements, 2011. **46**(1): p. 112-118.

[35] Ayres da Silva, A.L.M., et al., *Radon in Brazilian underground mines.* J Radiol Prot, 2018. **38**(2): p. 607-620.

[36] Ongori, J.N., et al., *Determining the radon exhalation rate from a gold mine tailings dump by measuring the gamma radiation.* J Environ Radioact, 2015. **140**: p. 16-24.